View metadata, citation and similar papers at core.ac.uk
brought to you by CORE
provided by Universiti Putra Malaysia Institutional Repository

International Food Research Journal 26(3): 781-791(June 2019)
Journal homepage: *http://www.ifrj.upm.edu.my*

Melting and crystallisation behaviour of soybean oil in blend with palm oil-based diacylglycerol

[1]Ong, C. R.-E., [2]Tang, T.-K., [3]Lee, Y.-Y., [4]Choong, T. S.-Y., [2,5]Lai, O.-M., [6]Kuan, C.-H. and [1*]Phuah, E.-T.

[1]*Department of Agricultural and Food Science, Universiti Tunku Abdul Rahman, Kampar, Perak, Malaysia*
[2]*Institute of Bioscience, Universiti Putra Malaysia, 43400 UPM Serdang, Selangor, Malaysia*
[3]*School of Science, Monash University Malaysia, 47500 Bandar Sunway, Selangor, Malaysia*
[4]*Department of Chemical Engineering, Faculty of Engineering, Universiti Putra Malaysia, 43400 UPM Serdang, Selangor, Malaysia*
[5]*Department of Bioprocess Technology, Faculty of Biotechnology and Biomolecular Sciences, Universiti Putra Malaysia, 43400 UPM Serdang, Selangor, Malaysia*
[6]*School of Biosciences, Faculty of Health and Medical Sciences, Taylors's University, 47500 Bandar Sunway, Selangor, Malaysia*

Article history

Received: 19 March, 2018
Received in revised form: 12 December, 2018
Accepted: 17 January, 2019

Keywords

Diacylglycerol
Palm oil
Soybean oil
Blending
Crystallisation and melting profile

Abstract

In the present work, the physicochemical properties namely fatty acid composition (FAC), iodine value (IV), acylglycerol content and thermal profiles of palm-based diacylglycerol (PDAG) in blend with soybean oil (SBO) at different concentrations (0-100 wt %) were evaluated. The Fourier-transform infrared spectroscopy (FTIR) spectra were determined at mid-infrared region to assign the functional groups. SBO exhibited the same absorption bands as PDAG except at wavelength of 1711, 1450, 1359, 850 and 779 cm^{-1}. This phenomenon indicated that the absorption frequency of the binary mixtures greatly depended on the composition of oil samples. IV of the oil blends was found to decrease from 131.09 ± 0.88 I_2/100 g to 51.55 ± 0.60 I_2/100 g with increasing PDAG concentrations due to the reduced degree of unsaturation. Generally, binary blends with an increasing PDAG concentration showed a decrease in linoleic acid (C18:2) as well as increase in oleic acid (C18:1) and palmitic acid (C16:0) contents. The DAG content for all the blends increased from 5.15 ± 1.40% to 87.80 ± 0.33% and TAG content decreased from 94.85 ± 1.40% to 12.20 ± 0.33% in tandem with increasing PDAG content. Incorporation of PDAG into SBO significantly affected the crystallisation and melting profiles of SBO.

© All Rights Reserved

Introduction

Diacylglycerol (DAG) is the esters of glycerol formed when two hydroxyl groups of the glycerol backbone are esterified with long-chain fatty acids (Flickinger and Matsuo, 2003). DAG can be found as a minor component up to 10% (w/w) in various edible fats and oils. The presence of small amount of DAG can significantly affect the physical properties of oils (D'Alonzo *et al*., 1982). With various modification approaches, the conventional fats and oils can undergo enzymatic and further purification process to increase their DAG content up to 80-90% (w/w) (Flickinger and Matsuo, 2003).

DAG oil is recognised as "Food for Specified Health Use" and GRAS (Generally Recognized as Safe) by FDA (Ng *et al*., 2014). The safety of DAG oils for human consumption has been proven by Marita and Soni (2009) through preclinical and toxicological studies. Most importantly, DAG diet was strongly reported to be capable of reversing the prevalence of obesity. As DAG is metabolised differently as compared to triacylglycerol (TAG), it increases β-oxidation of fatty acid, reduces postprandial lipemia and suppresses accumulation of visceral abdominal fat (Murase *et al*., 2001; Flickinger and Matsuo, 2003). The unique physicochemical properties of DAG are due to a slightly higher hydrophilicity of

*Corresponding author.
Email: phuahet@utar.edu.my

free hydroxyl group (Yasukawa and Katsuragi, 2004). Even though DAG has different metabolism, DAG-containing meal exhibits comparable bioavailability, energy value and equivalent digestibility as TAG-containing meal (Flickinger and Matsuo, 2003; Xu *et al*., 2015). DAG does not affect the fat digestion and absorption. Besides, DAG cooking oils have similar taste and texture as commercial TAG cooking oils. Despite several beneficial health benefits conferred by DAG, recent study reported that DAG is a precursor for the formation of 3-monochloropropane-1,2-diol (3-MCPD) which is a probable carcinogen produced during refining of fats and oils. Today, several approaches had been performed to reduce the 3-MCPD formation. Study showed that antioxidant with their free radical scavenger property is possible to mitigate the formation of 3-MCPD level in DAG oil (Xu *et al*., 2016).

Soybean- and canola-based DAG oils have been introduced in the United States and Japan market as functional cooking oils (Flickinger and Matsuo, 2003; Xu *et al*., 2007). Due to the beneficial effects of DAG on human health, various sources of fats and oils have been structurally modified to produce DAG oils which is inclusive of palm oil (Xu *et al*., 2015). Palm oil is one of the major fats and oils that approximately provides 28% of global edible oil output (Choo, 2012). The oil palms (*Elaeis guineensis* Jacq.) produce two different types of oils namely palm oil and palm kernel oil. Almost 90% of palm product is used in food products due to its desired properties and qualities (Idris *et al*., 1989). To provide value addition to the palm industry, several works have been performed to produce DAG from palm sources. Cheong *et al*. (2007) optimised the synthesis of DAG from palm sources *via* partial hydrolysis. Further, the unique properties of the synthesised palm-based diacylglycerol oil (PDAG) had been evaluated. PDAG was shown to have high slip melting points, broader solid fat content range and more compact crystalline network which is suitable for utilisation of plastic fats (Saberi *et al*., 2011; Xu *et al*., 2015). Saberi *et al*. (2011) suggested that a high concentration of PDAG (> 40%) could inhibit post-hardening problem that tends to give poor spreadability in spread. Similar study conducted by Cheong *et al*. (2007) also showed that PDAG demonstrated the ability to retard polymorphic transformation of PDAG-based margarine from β' to β during storage which enhances the shelf life of the margarine.

Application of vegetable oils in their original form is limited owing to their specific chemical composition (deMan, 1999). Therefore, food manufacturers often either physically or chemically modify the fats and oils in order to maximise its functions and usages (Chen *et al*., 2007). Oil blending is one the simplest modification processes to improve nutritional value and quality of the end product. It involves physical mixing of two or more oils with different characteristics (Li *et al*., 2014). Today, there is very little information available concerning the physicochemical effect of PDAG especially highly concentrated form of PDAG when blended with other sources of fats and oils. Blending of PDAG with various types of oils is important to extend its application and to reduce the production cost. Hence, it is vital to know the interaction between the PDAG and other oils to enhance their application in the food industry. The objectives of the present work were therefore to evaluate the effect of blending PDAG with soybean oil (SBO) at different ratios on the physicochemical properties of SBO oil namely FAC, IV, acylglycerol composition and thermal behaviour. Moreover, the functional groups of the binary blends were also indicated with Fourier transform infrared spectroscopy (FTIR) at mid-infrared region.

Materials and methods

Materials

Palm oil of IV 52 was provided by Golden Jomalina Sdn. Bhd., Teluk Panglima Garang, Selangor, Malaysia; while the commercial SBO was provided by Socma Trading (M) Sdn. Bhd., Subang Jaya, Selangor, Malaysia. Commercial immobilised lipase from *Candida antarctica* (Novozyme 435) was purchased from Novozyme A/S, Bagsvaerd, Denmark.

Preparation of PDAG oil

PDAG was first produced *via* enzymatic glycerolysis with Novozyme 435 lipase in a packed bed bioreactor at 65°C for 6 h. The molar ratio of glycerol/palm oil was 1:1, and the reaction was conducted through the stepwise addition of glycerol at interval time of 0, 0.5, 1, 1.5 and 2 h. The reaction mixture was pumped through the packed enzyme at a flow rate of 850 mL/min. The crude product was removed from the bottom of the packed bed bioreactor at the end of reaction, and stored at -18°C for purification.

Purification of PDAG was conducted using molecular distillation equipment model KD6 (UIC, Alzenau-Hoerstein, Germany). Two-step molecular distillation approach was employed to obtain high purity PDAG. The separation of glycerol, free fatty acid and monoacylglycerol (MAG) from the crude

product was done in the first distillation step at 200°C. The mixture of DAG and TAG collected from the residue vessel was used for second distillation step at 250°C where the DAG was segregated from the TAG and collected from the distillate vessel. The following operating conditions were used for both purification steps: evaporator vacuum, 0.001 mbar; feeding rate, 1.3 L/h; condenser temperature, 85°C; feeding tank temperature, 75°C; and roller speed, 280 rpm.

High purity PDAG was then refined, bleached and deodorised in a 20 L pilot-scale refining plant under vacuum condition (1 - 2 mmHg). Refining was carried out using 0.1% phosphoric acid at 90°C for 30 min. Subsequently, bleaching was performed at 100°C for 30 min using 1% activated bleaching earth. Finally, deodorisation was conducted at 200°C for 2 h to obtain the final product which was a purified PDAG with more than 80 wt % DAG.

Preparation of oil blends

Eleven blends of PDAG with SBO in various ratios were prepared based on the percentage of total weight (wt %) and denoted as blends A-K. The concentrations of PDAG ranged from 0% to 100% with 10% increment (w/w). 100% w/w of PDAG and 100% w/w of SBO served as controls. The oils were melted at 70°C and stirred vigorously for 5 min, then blended for 2 min with low rotation speed to destroy the crystals. All blends were prepared in duplicate and stored at -20°C before analysis.

Fatty acid composition (FAC)

The FAC was determined by fatty acid methyl esters (FAME) using gas chromatography, GC-2010 Shimadzu (Shimadzu Corporation, Japan) following the method described by Ng *et al*. (2014). Approximately 100 mg of oil blend was first dissolved in 5 mL of hexane before 250 µL of 0.5 M sodium methoxide reagent was added. The mixture was vortexed for 1 min and paused for every 10 s. The mixture was then added with 5 mL of saturated sodium chloride, shook vigorously for 15 s and allowed to settle for 10 min. Next, 1 µL of the top layer of FAME was filtered before injected into the gas chromatography (GC). The GC was equipped with a flame ionisation detector (FID), biodiesel EN14103 FAME analysis fused silica column (30 m × 0.32 mm and 0.25 µm) (Agilent, USA). The injector and FID temperate were set at 220°C. Helium was used as carrier gas at 23 mL/min flow rate and nitrogen was used as makeup gas at 20 mL/min. The initial temperature of column was 115°C and programmed to 180°C at a rate of 8°C/min. The fatty acid was identified by comparing the retention time of 37 FAME standards. The FAC was then quantified using peak area normalisation technique.

Iodine value (IV)

The IVs of blends were obtained based on AOCS method (AOCS, 2009). Firstly, 20 mL of cyclohexane was added to 0.5 g of sample to dilute the sample. Then, 25 mL of Wijs solution (ICl) was added to halogenate the double bonds and placed in dark area for 1 h. After that, 20 g of potassium iodine and 100 mL of distilled water were reacted with the mixtures. The free iodine (I_2) was measured by titration with 24.9 g/L of $Na_2S_2O_3 \cdot 5H_2O$ with 1 g/100 mL of starch indicator. The IV of each blend was determined in duplicate. The absorbed I_2/g sample was calculated using Eq. 1 (Norizzah *et al*., 2014):

$$IV = [12.69\ M\ (Vb - Vs)] / W \quad \text{(Eq. 1)}$$

where M = molarity of sodium thiosulphate solution; Vb = volume of sodium thiosulphate solution used for blank test in mL; Vs = volume of sodium thiosulphate used for sample test in mL; and W = sample weight in g.

Acylglycerol composition

The acylglycerol compositions of samples were determined with high performance liquid chromatography (HPLC) (Yeoh *et al*., 2014). The HPLC system (Hewlett-Packard, US) was equipped with Agilent 1100 HPLC system, refractive index detector and quaternary pump. The column used was Phenomenex Gemini® 5 µm C_{18} 110 Å, LC, column 150 × 4.60 mm ID with particle size of 5 µm. The mobile phase of HPLC consisted of pre-mixed acetonitrile and acetone in channels A (37.5:62.5% v/v), at a flow rate of 0.5 mL/min. The oven temperature was set at 35°C. 50 µL of sample was dissolved into 950 µL of acetone and then 10 µL of sample was filtered and injected into the HPLC. Each blend was measured in duplicate and peak area normalisation method was used to quantify the DAG (Lo, 2007). The compositions of MAG, DAG and TAG were determined as percentage of the total acylglycerol content of the sample. Based on area normalisation method, the percentage of DAG was calculated using Eq. 2:

$$\%\ DAG = [DAG / (MAG + DAG + TAG)] \times 100\% \quad \text{(Eq. 2)}$$

Thermal behaviour

The crystallisation and melting behaviours of the oil samples were determined by differential scanning calorimetry (DSC) (Mettler Toledo International Inc., Switzerland) (Ng *et al*., 2014). An empty and hermetically sealed DSC aluminium pan was used as control. Approximately 7 mg of samples were weighed into aluminium pans and covered. The samples were heated at 80°C for 10 min to destroy crystal nuclei, and then cooled to -30°C at a rate of 5°C/min and maintained for 10 min. Then, the sample was heated to 80°C at 5°C/min and maintained for 10 min. The cooling and heating thermograms for each sample were recorded using normalised thermogram. The DSC parameters were obtained in duplicate with DSC Data Analysis software.

Infrared spectra acquisition (FTIR)

The fingerprints of oil blends were determined with PerkinElmer FTIR Spectrum RX1 (Thermo Fisher Scientific, US) (Ng *et al*., 2014). The spectra of binary blends at the mid-infrared region (4400-660 cm^{-1}) were determined under ambient temperature. A drop of oil was sandwiched between the NaCl salt plate and placed in cell holder. The FTIR spectra took 32 scans at 4 cm^{-1} resolution. Anhydrous chloroform was used to clean the salt plate after each measurement. The backgrounds were collected before every measurement to ensure the salt plate was cleaned properly. Each sample was repeated in duplicate and the absorbance values were recorded.

Statistical analysis

All measurements were conducted in duplicate (n = 2) and presented as the arithmetic means with standard deviation. SPSS software was used to analyse the data by using one-way analysis of variance (ANOVA) and Tukey's Multiple Comparison test to determine the significant differences among the means. The *p* values of less than 0.05 were reported as significant.

Results and discussion

Fatty acid compositions (FAC)

Table 1 shows the FAC as well as IV of PDAG, SBO and their binary blends. The dominant fatty acids for all the samples were palmitic (C16:0), oleic (C18:1) and linoleic (C18:2) acids. PDAG contained 44.57 ± 0.00% of C16:0, 38.83 ± 0.18% of C18:1 and 11.93 ± 0.11% of C18, whereas SBO consisted of 10.47 ± 0.01% of C16:0, 23.30 ± 0.08% of C18:1 and 52.31 ± 0.18% of C18:2. PDAG contained higher amount of saturated fatty acid (SAFA) as compared to SBO with 49.23 ± 0.08% and 14.92 ± 0.01%, respectively. The results were similar with the work of Saberi *et al*. (2011) with 45.6% of C16:0 and 38.4% of C18:1. On the other hand, the SBO contained high amounts of unsaturated fatty acid, USAFA, (52.31 ± 0.18% C18:2 and 23.30 ± 0.08% C18:1), which agrees with the study of Li *et al*. (2014) with 53.03% of C18:2 and 22.68% of C18:1.

Addition of PDAG to SBO significantly ($p < 0.05$) increased the composition of C16:0 and C18:1 from 10.47 ± 0.01% to 41.93 ± 0.02% and 23.30 ± 0.08% to 37.04 ± 0.03%, respectively. A decreasing trend was noticed in C18:2 with increasing PDAG concentrations. Similarly, a decreasing trend in linolenic (C18:3) acid from 9.47 ± 0.25% to 0.06 ± 0.00% was observed with increasing concentrations of PDAG. This might have occurred as a result of the incorporation of PDAG, which is high in SAFA into SBO, which decreased the USAFA content in SBO. In addition, the binary blends comprised minor amount (< 4%) of stearic (C18:0) acid and trace amount (< 1%) of lauric (C12:0), myristic (C14:0) and arachidonic (C20:0) acids.

The USAFA and SAFA contents of SBO were 85.08 ± 0.01% and 14.92 ± 0.01%, respectively. Tan and Che Man (2000) obtained similar results for SBO. PDAG had a higher USAFA content (50.77%) and a lower SAFA content (49.23%). The increasing PDAG content significantly decreased USAFA content and increased SAFA content. The changes in acylglycerol composition are the main reason for changes in FAC rather than the difference in chemical composition (Miklos *et al*., 2013; Ng *et al*., 2014). Moreover, the FAC of acylglycerol fraction will not be altered by enzymatic glycerolysis and purification process (Cheong *et al*., 2009; Saberi *et al*., 2011; Ng *et al*., 2014).

Iodine value

IV is a measure of the degree of unsaturation of fat and oil which is expressed as iodine absorbed by 100 parts of substance by weight (Abdul Azis *et al*., 2011). Table 1 shows the IV of SBO, PDAG and their binary blends. A low IV indicates high degree of saturation and vice versa. The low IV of palm-based oil products is due to the high levels of saturated and monounsaturated fatty acids which can be seen in PDAG oil (Ng *et al*., 2014). In contrast, the high IV of SBO could be attributed to the high proportion of USAFA (Cheong *et al*., 2009). In general, IV decreased significantly ($p < 0.05$) with increasing PDAG contents and vice versa. The decreased in IV upon addition of PDAG into SBO indicated the increase in the SAFA content in the blend which was contributed by the PDAG.

Table 1. The fatty acid compositions, acylglycerol compositions and iodine values of PDAG:SBO blends.

FA (%)	A (0:100)	B (10:90)	C (20:80)	D (30:70)	E (40:60)	F (50:50)	G (60:40)	H (70:30)	I (80:20)	J (90:10)	K (100:0)
C12:0	$0.23^{b} \pm 0.00$	$0.22^{b} \pm 0.00$	$0.21^{b} \pm 0.00$	$0.20^{b} \pm 0.01$	$0.51^{c} \pm 0.00$	$0.46^{d} \pm 0.02$	$0.42^{c} \pm 0.02$	$0.40^{c} \pm 0.00$	$0.14^{a} \pm 0.00$	$0.13^{a} \pm 0.00$	$0.12^{a} \pm 0.00$
C 14:0	$0.07^{a} \pm 0.00$	$0.16^{a} \pm 0.01$	$0.23^{ab} \pm 0.00$	$0.34^{ab} \pm 0.00$	$0.50^{bc} \pm 0.09$	$0.66^{cd} \pm 0.19$	$0.65^{cd} \pm 0.05$	$0.77^{cde} \pm 0.05$	$0.85^{de} \pm 0.04$	$0.91^{de} \pm 0.01$	$1.06^{e} \pm 0.11$
C16:0	$10.47^{a} \pm 0.01$	$13.67^{b} \pm 0.02$	$16.85^{c} \pm 0.03$	$20.34^{d} \pm 0.16$	$23.92^{e} \pm 0.09$	$27.77^{f} \pm 0.35$	$30.83^{g} \pm 0.02$	$34.97^{h} \pm 0.01$	$38.27^{i} \pm 0.36$	$41.93^{j} \pm 0.02$	$44.57^{k} \pm 0.00$
C18:0	$3.85^{b} \pm 0.00$	$3.82^{b} \pm 0.01$	$3.82^{b} \pm 0.01$	$3.80^{b} \pm 0.01$	$3.82^{b} \pm 0.01$	$3.78^{b} \pm 0.08$	$3.77^{b} \pm 0.06$	$3.64^{b} \pm 0.23$	$3.32^{a} \pm 0.04$	$3.32^{a} \pm 0.01$	$3.22^{a} \pm 0.04$
C18:1	$23.30^{a} \pm 0.08$	$24.72^{b} \pm 0.12$	$26.14^{c} \pm 0.00$	$27.67^{d} \pm 0.24$	$29.30^{e} \pm 0.08$	$30.73^{f} \pm 0.66$	$32.40^{g} \pm 0.42$	$34.72^{h} \pm 0.15$	$35.64^{i} \pm 0.03$	$37.04^{j} \pm 0.03$	$38.83^{k} \pm 0.18$
C18:2	$52.31^{k} \pm 0.18$	$48.48^{j} \pm 0.40$	$44.25^{i} \pm 0.03$	$40.21^{h} \pm 0.25$	$36.20^{g} \pm 0.07$	$32.11^{f} \pm 0.62$	$28.10^{e} \pm 0.25$	$24.00^{d} \pm 0.05$	$21.39^{c} \pm 0.37$	$16.34^{b} \pm 0.01$	$11.93^{a} \pm 0.11$
C18:3	$9.47^{e} \pm 0.25$	$8.64^{de} \pm 0.50$	$8.21^{de} \pm 0.04$	$7.15^{d} \pm 0.69$	$5.04^{c} \pm 0.02$	$3.82^{bc} \pm 0.78$	$3.20^{b} \pm 0.71$	$0.89^{a} \pm 0.02$	$0.11^{a} \pm 0.00$	$0.06^{a} \pm 0.00$	$0.01^{a} \pm 0.00$
C20:0	$0.30^{a} \pm 0.01$	$0.29^{a} \pm 0.00$	$0.29^{a} \pm 0.00$	$0.29^{a} \pm 0.01$	$0.71^{d} \pm 0.01$	$0.67^{cd} \pm 0.03$	$0.63^{bc} \pm 0.01$	$0.61^{b} \pm 0.01$	$0.28^{a} \pm 0.01$	$0.27^{a} \pm 0.00$	$0.26^{a} \pm 0.00$
USAFA	$85.08^{k} \pm 0.01$	$81.84^{j} \pm 0.02$	$78.60^{i} \pm 0.01$	$75.03^{h} \pm 0.19$	$70.54^{g} \pm 0.18$	$66.66^{f} \pm 0.50$	$63.70^{e} \pm 0.05$	$59.61^{d} \pm 0.18$	$57.14^{c} \pm 0.34$	$53.44^{b} \pm 0.01$	$50.77^{a} \pm 0.06$
SAFA	$14.92^{a} \pm 0.01$	$18.16^{b} \pm 0.01$	$21.40^{c} \pm 0.01$	$24.97^{d} \pm 0.19$	$29.46^{e} \pm 0.18$	$33.34^{f} \pm 0.51$	$36.30^{g} \pm 0.06$	$40.39^{h} \pm 0.18$	$42.86^{i} \pm 0.35$	$46.56^{j} \pm 0.01$	$49.23^{k} \pm 0.08$
IV	$131.09^{k} \pm 0.88$	$114.89^{j} \pm 0.51$	$107.98^{i} \pm 0.70$	$101.96^{h} \pm 0.50$	$98.28^{g} \pm 0.62$	$91.33^{f} \pm 0.51$	$84.30^{e} \pm 0.74$	$77.32^{d} \pm 0.83$	$73.02^{c} \pm 0.40$	$66.68^{b} \pm 0.46$	$51.55^{a} \pm 0.60$
TAG	$94.85^{h} \pm 1.40$	$79.35^{g} \pm 1.91$	$75.85^{g} \pm 0.21$	$69.52^{f} \pm 1.94$	$57.93^{e} \pm 1.74$	$46.88^{d} \pm 2.57$	$44.15^{d} \pm 0.30$	$35.61^{c} \pm 0.88$	$27.32^{b} \pm 0.53$	$21.24^{b} \pm 2.50$	$12.20^{a} \pm 0.33$
DAG	$5.15^{a} \pm 1.40$	$20.65^{b} \pm 1.91$	$24.15^{b} \pm 0.21$	$30.48^{c} \pm 1.94$	$42.07^{d} \pm 1.74$	$53.12^{e} \pm 2.57$	$55.85^{e} \pm 0.30$	$64.39^{f} \pm 0.88$	$72.68^{g} \pm 0.53$	$78.76^{g} \pm 2.50$	$87.80^{h} \pm 0.33$

Data are means ± SD of two replicates ($n = 2$). Samples A to K represent the percentage of PDAG increased from 0 to 100%, while the percentage of SBO decreased from 100 to 0%. Means with different superscripts in each row were significantly different ($p < 0.05$).

Acylglycerol composition

Each fat and oil have their own unique TAG profiles (Tsimidou *et al*., 1987). The major composition in SBO was TAG (94.85 ± 1.40%) and minor amount of DAG (5.15 ± 1.40%). The result was slightly different with Júnior *et al*. (2013) which reported 97.46% of TAG and 2.54% of DAG. This might be due to SBO from different geological locations. PDAG had a higher DAG content (87.80 ± 0.33%) and lower TAG content (12.20 ± 0.33%). The acylglycerol contents were slightly different with the result reported by Saberi *et al*. (2011) which were 90.02% of DAG and 9.98% of TAG. This might be due to the difference in parameter of enzymatic glycerolysis process of PDAG as reported by the authors. The DAG content of binary blends obviously increased in tandem from 20.65 ± 1.91% to 78.76 ± 2.50% with increasing PDAG contents. An opposite trend was observed for TAG amount in the blended oils, which showed reductions from 79.35 ± 1.91% to 21.24 ± 2.50% corresponding to the increase in PDAG concentrations. This phenomenon showed the interaction between the blended oils.

Thermal behaviour

Dynamic crystallisation behaviour

Figure 1 (a-b) compares the dynamic crystallisation profiles of PDAG blends with SBO in different concentrations while Table 2 shows the summarised parameters. Crystallisation properties are important parameters which influence the network structure thereby affecting functionality, organoleptic, rheological and textural behaviours of the plastic fats (Marangoni and Lencki, 1998; Rousseau *et al*., 1998). Crystallisation thermogram is simpler than the melting thermogram as it is only affected by the chemical composition of oil instead of the primary crystallisation state (Tan and Che Man, 2002). The crystallisation behaviour of fat and oil depends on the variables (i.e., cooling rate), interactions among chemical and physical variables (i.e., ratio of DAG/TAG, melting profile, structural compatibility among DAG and TAG) (Reyes-Hernández *et al*., 2007). The initial crystallisation was related to the rearrangement of molecules while the aggregation and compression of molecules indicated the ending of crystallisation

(Tan and Che Man, 2002). PDAG (47.76°C) had a higher crystallisation onset temperature (T_{oc}) than SBO (-8.57 ± 0.01°C) because of the high SAFA content and low USAFA content in the PDAG (Saberi *et al*., 2011). SBO had only one transition peak at -9.71 ± 0.06°C which disagreed with Tan and Che Man (2000) who revealed three exothermic peaks. The addition of PDAG to SBO revealed new peak at the initial stage of crystallisation indicating the disturbance of nucleation process (Miklos *et al*., 2013). The effect of PDAG on different growth behaviours of crystal network depends on the concentration added (Saberi *et al*., 2011; Ng *et al*., 2014). PDAG had three transition peaks at wide temperature range with T_{oc} at 47.76 ± 0.16°C and T_{fc} at -10.03 ± 0.57°C. Xu *et al*. (2016) reported PDAG with four transition peaks of crystallisation curve with T_{oc} at 31.75°C and T_{fc} at -10.67°C. This might be due to the higher cooling rate of 10°C/min in the previous study, causing the temperature shifted to a lower temperature.

A lower exotherm temperature was related to the crystallisation of olein fraction, whereas a higher exotherm temperature was attributed to the crystallisation of stearin fraction (Tan and Che Man, 2002). The intensity of P1 shifted towards lower temperature for oil blends containing 10% to 40% of PDAG indicated retardation or disturbance of crystal growth. In contrast, nucleation and crystal growth was promoted in the blends with a higher concentration of PDAG (Miklos *et al*., 2013). It has been reported that the addition of 2% and 5% of PDAG decreased the crystallisation rate and crystal growth mode of palm oil; while 30% and 50% of PDAG significantly increased crystallisation and nucleation rate of the binary systems (Saberi *et al*., 2011). The compact and homogeneous microstructure of needle-like crystals of PDAG is the reason behind the rapid crystallisation (Xu *et al*., 2015). On the contrary, the retardation effect corresponded to β_1 form of PDAG. In fact, a small amount of PDAG may greatly impart steric hindrance and thus prevent more crystal packing (Saberi *et al*., 2011). This is due to the limited number of growth sites on nuclei (Boistelle, 1988). The addition of PDAG to SBO increased the transition temperature of P3 from 27.71 ± 0.88°C to 46 ± 0.00°C which might be due to co-crystallisation of DAG with high-melting fraction of TAG components or crystallisation-inducing acylglycerol components (i.e., dipalmitin and 3-dipalmitoyl-1-oleoyl-glycerol) (Xu *et al*., 2015). Moreover, the peak area of P3 which was larger than that of P2 indicated that the quantity of crystal fraction formed at third stage crystallisation was larger than that at second stage crystallisation (Saitou *et al*., 2012). Three different exothermic peak heights were noticed in the binary blends. Generally, the peak heights of major crystallisation event revealed an increase from 0.05 ± 0.88 0.00 W/g to 1.75 ± 0.88 0.14 W/g (Table 2). Additionally, the ΔH_c of SBO:PDAG blends significantly (p < s0.05) increased with increasing PDAG contents, indicating an increase in molecules number and more energy release during crystallisation by the binary systems (Humphrey *et al*., 2004).

Dynamic melting behaviour

The melting profiles of binary mixtures are shown in Figure 1 (c-d) whereas the summarised parameters are shown in Table 3. The DSC melting profile can be classified into three melting fractions; low (LMF), medium (MMF) and high (HMF) melting fractions (Latip *et al*., 2013).

The three well-defined peaks in melting profiles of PDAG could be related to the three major DAG groups (i.e., disaturated, monounsaturated and diunsaturated DAG) (Saberi *et al*., 2011). In this finding, the LMF had one peak (P1) and MMF had two peaks (P2 and P3), while HMF had two peaks (P4 and P5). The separate endothermic peaks were related to polymorphic transition as well as the low and high melting components of a fat or oil (deMan *et al*., 1989). The PDAG in the present work had a similar melting point to that reported by Saberi *et al*. (2011) which was 57.92°C and 57.8°C, respectively. The melting point greatly depends on the strength of hydrogen bonding of hydroxyl group and fatty acid chain arrangement (Xu *et al*., 2015). This finding had a higher HMF (55.96 ± 0.06°C) and a lower LMF (3 ± 0.00°C) as compared to the study conducted by Xu *et al*. (2015) at 45.9°C and 5.1°C, respectively. Saberi *et al*. (2011) revealed PDAG with two endothermic peaks at 24.78°C and 53.56°C. SBO had a lower P1 (-11.59°C) in LMF region than PDAG (3°C) due to the high level of polyunsaturated component in SBO. Tan and Che Man (2000) outlined SBO with four transition temperatures in the endothermic event at -41.25°C, -32.82°C, -26.12°C and -14.30°C. The different patterns in melting curve of PDAG and SBO might relate to their acylglycerol contents (Saberi *et al*., 2011).

Obviously, the melting behaviour of SBO was greatly altered with the addition of PDAG. The addition of PDAG to SBO caused the peak height of major melting event (P5) to gradually increase from 0.01 ± 0.00 W/g to 0.44 ± 0.01 W/g (Table 3). The high and sharp melting peaks of oil blends with a higher PDAG concentration at P2 and P5 indicated more crystal growth and less nucleation site (Latip

et al., 2013). The increasing trends of ΔH_m were parallel with the increasing SAFA and disaturated DAG contents in the SBO:PDAG blends (Saberi *et al*., 2011). Consequently, PDAG (58.04 ± 1.03 J/g) had a higher ΔH_m which indicated that more energy was needed to melt the DAG-oil as compared to SBO (15.12±0.86 J/g).

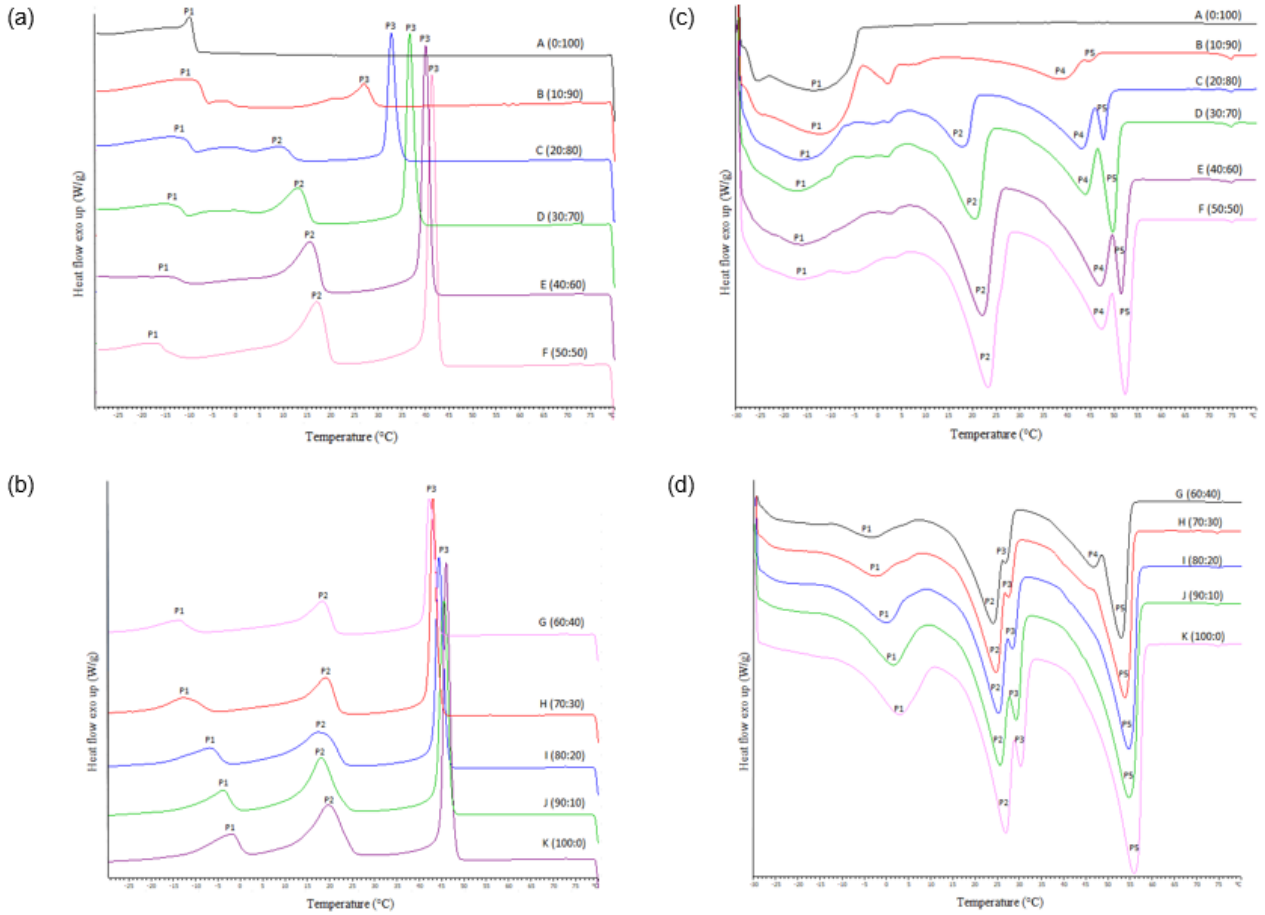

Figure 1: (a)-(b) dynamic crystallisation profile, (c)-(d) dynamic melting profile, of palm-based diacylglycerol (K), soybean oil (A) and their binary blends (B-J).

Table 2. Crystallisation onset (T_{oc}), crystallisation offset (T_{fc}), crystallisation enthalpy (ΔH_c) and dynamic crystallisation profiles of PDAG, SBO and their binary blends at 5°C/min intervals.

PDAG: SBO	Transition temperature (°C)			Peak height (W/g) of P_3	T_{oc} (°C)	T_{fc} (oC)	ΔH_c (J/g)
	P_1	P_2	P_3				
A (0:100)	-9.71^{f} ± 0.06	-	-	-	-8.57^{a} ± 0.01	-11.69^{g} ± 0.14	1.51^{a} ± 0.16
B (10:90)	-10.17^{f} ± 0.24	-	27.71^{a} ± 0.88	0.05^{a} ± 0.00	29.96^{b} ± 0.87	-26.52^{a} ± 0.42	10.97^{b} ± 0.78
C (20:80)	-12.75^{e} ± 0.11	9.63^{a} ± 0.06	32.88^{b} ± 0.18	0.36^{b} ± 0.00	34.58^{c} ± 0.18	-25.89 ^{ab} ± 0.43	15.57^{c} ± 1.11
D (30:70)	-14.42^{c} ± 0.00	13.25^{b} ± 0.24	36.80^{c} ± 0.18	0.53^{bc} ± 0.01	38.55^{d} ± 0.30	-24.35^{bc} ± 0.41	20.21^{d} ± 0.06
E (40:60)	-15.80^{b} ± 0.18	15.84^{c} ± 0.23	40.21^{d} ± 0.30	0.65^{cd} ± 0.04	41.73^{e} ± 0.30	-23.91^{c} ± 0.11	25.85^{e} ± 1.43
F (50:50)	-16.42^{a} ± 0.00	17.25^{cd} ± 0.24	41.50^{e} ± 0.24	0.81^{de} ± 0.01	43.10^{f} ± 0.24	-23.50^{c} ± 0.18	31.58^{f} ± 0.62
G (60:40)	-13.84^{d} ± 0.12	18.38^{de} ± 0.18	42.34^{ef} ± 0.12	0.87^{e} ± 0.01	44.41^{g} ± 0.06	-21.65^{d} ± 0.06	42.38^{g} ± 0.83
H (70:30)	-12.83^{e} ± 0.00	19.25^{f} ± 0.11	43.04^{f} ± 0.06	1.34^{f} ± 0.06	44.57^{g} ± 0.16	-18.90^{e} ± 0.71	48.15^{h} ± 0.25
I (80:20)	-6.88^{g} ± 0.18	18.38^{de} ± 0.77	44.38^{g} ± 0.06	1.29^{f} ± 0.04	46.26^{h} ± 0.11	-15.86^{f} ± 0.64	58.70^{i} ± 1.28
J (90:10)	-3.75^{h} ± 0.11	18.21^{de} ± 0.18	45.63^{gh} ± 0.18	1.36^{f} ± 0.02	47.27^{hi} ± 0.16	-10.18^{g} ± 0.52	69.95^{j} ± 1.79
K (100:0)	-2.00^{i} ± 0.00	19.67^{f} ± 0.00	46.00^{h} ± 0.00	1.75^{g} ± 0.14	47.76^{i} ± 0.16	-10.03^{g} ± 0.57	80.04^{k} ± 1.10

Data are means ± SD of two replicates (n = 2). Means with different superscripts in each column were significantly different ($p < 0.05$).

Table 3. Melting onset (T_{om}), melting offset (T_{fm}), melting enthalpy (ΔH_m) and dynamic melting profiles of PDAG, SBO and their binary blends with 5°C/min intervals.

PDAG:SBO	Transition temperature (°C)					Peak height of P_5 (W/g)	T_{om} (°C)	T_{fm} (°C)	ΔH_m (J/g)
	P_1	P_2	P_3	P_4	P_5				
A (0:100)	-11.59^{d} ± 0.23	-	-	-	-	-	-29.86^{a} ± 0.01	-4.06^{a} ± 0.05	15.12^{a} ± 0.86
B (10:90)	-12.17^{cd} ± 0.23	-	-	39.00^{a} ± 0.47	45.13^{a} ± 0.29	0.01^{a} ± 0.00	-29.10^{a} ± 0.13	46.48^{b} ± 0.16	18.52^{b} ± 1.17
C (20:80)	-15.42^{bcd} ± 0.76	18.17^{a} ± 0.23	-	43.09^{b} ± 0.12	47.67^{b} ± 0.00	0.05^{b} ± 0.00	-29.05^{a} ± 0.06	48.88^{c} ± 0.01	20.34^{b} ± 1.47
D (30:70)	-18.04^{abc} ± 0.06	20.67^{b} ± 0.00	-	43.96^{b} ± 0.06	49.76^{c} ± 0.13	0.12^{c} ± 0.00	-29.00^{a} ± 0.13	51.09^{d} ± 0.04	25.52^{c} ± 0.37
E (40:60)	-21.21^{ab} ± 4.77	22.17^{c} ± 0.00	-	46.42^{c} ± 0.59	51.42^{d} ± 0.12	0.11^{c} ± 0.01	-28.95^{a} ± 0.04	53.01^{e} ± 0.23	29.71^{d} ± 0.37
F (50:50)	-23.83^{a} ± 1.06	23.34^{d} ± 0.12	-	46.79^{c} ± 0.30	52.34^{e} ± 0.12	0.18^{d} ± 0.01	-28.82^{a} ± 0.38	54.12^{f} ± 0.13	30.30^{d} ± 0.30
G (60:40)	-3.33^{e} ± 0.00	23.96^{e} ± 0.06	27.29^{a} ± 0.06	46.94^{c} ± 0.74	53.13^{f} ± 0.06	0.23^{e} ± 0.01	-9.31^{b} ± 0.54	55.00^{f} ± 0.02	31.09^{d} ± 0.49
H (70:30)	-2.38^{ef} ± 0.29	24.63^{f} ± 0.06	27.96^{b} ± 0.06	-	53.96^{g} ± 0.06	0.30^{f} ± 0.01	8.12^{bc} ± 0.45	55.76^{g} ± 0.07	33.36^{d} ± 0.08
I (80:20)	0.04^{ef} ± 0.30	25.09^{g} ± 0.12	28.67^{c} ± 0.00	-	54.67^{h} ± 0.00	0.36^{g} ± 0.01	-6.99^{cd} ± 0.92	56.72^{h} ± 0.00	45.13^{e} ± 1.81
J (90:10)	1.63^{ef} ± 0.06	25.54^{h} ± 0.06	29.58^{d} ± 0.00	-	54.88^{h} ± 0.06	0.38^{g} ± 0.01	-6.90^{cd} ± 1.07	57.15^{hi} ± 0.08	51.48^{f} ± 1.67
K (100:0)	3.00^{f} ± 0.00	26.75^{i} ± 0.00	30.54^{e} ± 0.06	-	55.96^{i} ± 0.06	0.44^{h} ± 0.01	-5.02^{d} ± 1.27	57.92^{i} ± 0.05	58.04^{g} ± 1.03

Data are means ± SD of two replicates (n = 2). Means with different superscripts in each column were significantly different (p < 0.05).

Fourier transform infrared (FTIR) spectra

FTIR spectra is a fingerprint technique that allows differentiation among fats and oils (Rohman *et al*., 2012). Figure 2 shows the FTIR spectra of PDAG, SBO and their binary blends with their assigned bands for both PDAG and SBO spectra. The FTIR spectra were measured at mid-infrared region (4400-650 cm^{-1}) and comprised characteristic bands that were related to specific function group at different frequencies and intensities. The assignment of functional group and mode of vibration for IR absorption were: 3468 (-O-C=O stretch), 3006 (cis =C-H stretch), 2953 ($-CH_3$ asymmetrical stretch), 2853 ($-CH_2$ symmetrical stretch), 2677 (-C=O stretch), 1746 and 1711 (ester or acid -C=O stretch), 1654 (cis –C=C stretch), 1465 ($-CH_2$ scissoring), 1450 ($-CH_3$ asymmetric bending), 1417 (cis =C-H rocking), 1400 (=C-H bending), 1377 ($-CH_3$ symmetrical bending), 1359 (-O-H in plane), 1290-1006 (-C-O stretch), 914 (cis –HC=CH- bending out of plane), 850 ($=CH_2$ wagging), 779 (-C-H bending out of plane) and 722 cm^{-1} (cis –HC=CH- bending out of plane) (Guillen and Cabo, 1997). Apparently, the SBO:PDAG blends increased in frequencies and band intensities of spectra with increasing concentrations of PDAG. Several large peaks were consistently and clearly observed at 3009, 2972, 2854, 1747, 1377, 1163 and 723 cm^{-1} over the samples. The pattern of SBO spectra is similar to infrared spectra reported by Petrović (2008). SBO spectrum had a sharper band at 3009 cm^{-1} as compared to PDAG spectrum which indicated that the composition of linoleic acyl group of SBO was higher than PDAG. However, SBO showed a smaller band at 3468 cm^{-1} which was attributed to glyceride ester carbonyl (-O-C=O) absorption than PDAG. Besides, some bands were only detected in PDAG spectrum but not in SBO spectra including 1711 (I), 1450 (II), 1359 (III), 850 (IV) and 779 cm^{-1} (V). As a result, the increase in the concentration of PDAG in SBO led to an increase in these peak intensities. The change of absorbance in these bands could therefore be used for the quantification of PDAG in the binary blend based on the calibration model developed.

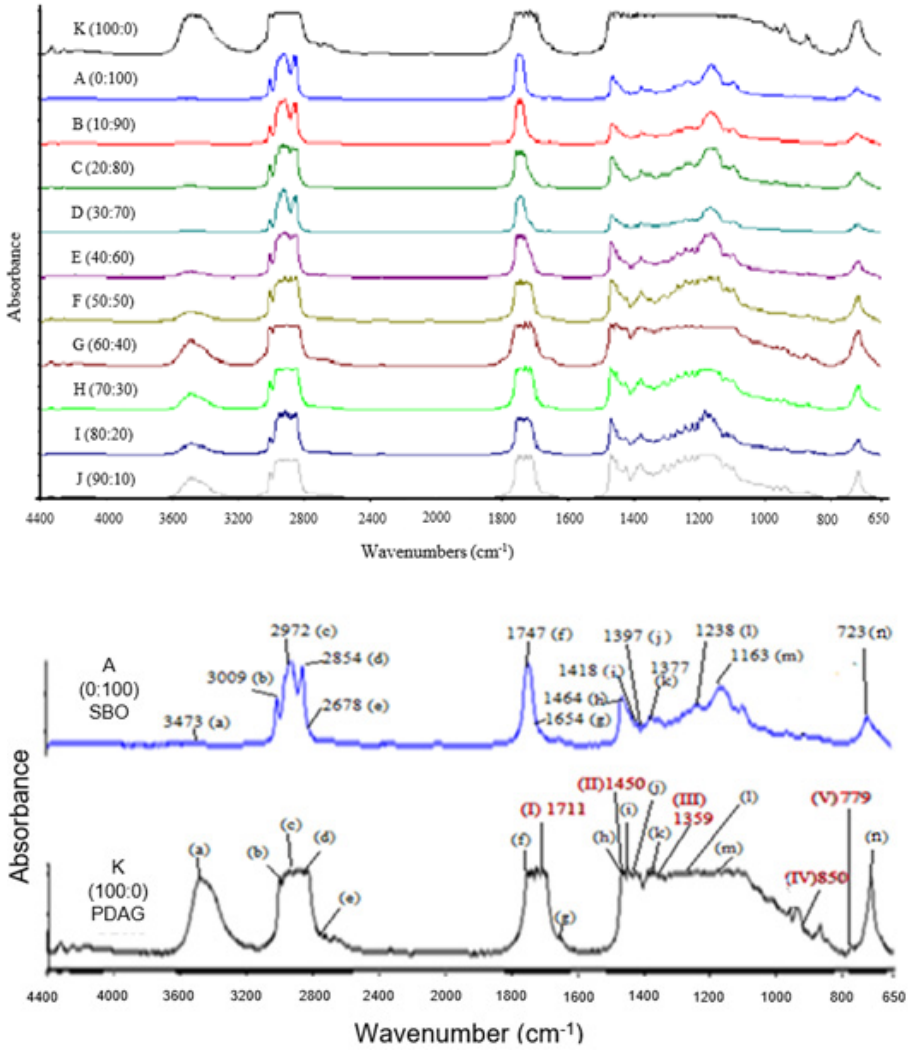

Figure 2: The FTIR spectra of PDAG (Blend K), SBO (Blend A) and their binary blends (Blend B-J) at frequency of 4400 – 650 cm^{-1}. The numbers of bands assigned are referred to Guillen and Cabo (1997).

Conclusion

The present work revealed that blending could modify the physicochemical properties but not the chemical properties of fats and oils. Each of the nine SBO:PDAG blends had different FAC, IV, acylglycerol content, thermal properties and infrared spectrum. Palmitic, oleic and linoleic acids were the major fatty acids found in the binary systems. The IV of oil blends significantly decreased with increasing PDAG concentrations due to the increase in saturated and monounsaturated fatty acids contents contributed by PDAG. Meanwhile, the addition of PDAG to SBO also increased the DAG content and reduced the TAG content of the blend. A high concentration of PDAG increased the nucleation and crystallisation rate of SBO; while low concentration of PDAG revealed inhibitory effect. The SBO:PDAG blends had different pattern of melting profiles based on the PDAG concentration; while the SBO only showed a transition peak at LMF region. The melting point of binary oils increased with increasing concentration of PDAG due to the increasing SAFA and disaturated DAG contents. Moreover, several large peaks of infrared spectra were consistently observed in the systems. The binary blends of SBO:PDAG have the potential to be used as hardstock for margarine to deliver beneficial health effects.

Acknowledgement

The authors would like to acknowledge Sime Darby Research Sdn. Bhd. for their financial and technical support. The authors would also like to thank Universiti Tunku Abdul Rahman (UTAR) for the research funding.

References

Abdul Azis, A., Mohamud, Y., Roselina, K., Boo, H. C., Nyuk, L. C. and Che Man, Y. B. 2011. Rheological, chemical and DSC thermal characteristics of different types of palm oil/palm stearin-based shortenings. International Food Research Journal 18(1): 189-200.

American Oil Chemist's Society (AOCS). 2009. Official methods and recommended practices of the American Oil Chemists' Society. 6th ed. Champaign: American Oil Chemist's Society Press.

Boistelle, R. 1988. Fundamentals of nucleation and crystal growth. In Garti, N. and Sato, K. (eds.). Crystallization and polymorphism of fats and fatty acids, p. 189-226. New York: Marcel Dekker.

Chen, C. W., Chong, C. L., Ghazali, H. M. and Lai, O. M. 2007. Interpretation of triacylglycerol profiles of palm oil, palm kernel oil and their binary blends. Food Chemistry 100(1): 178-191.

Cheong, L.-Z., Tan, C.-P., Long, K., Yusoff, M. S. A. and Lai, O.-M. 2009. Physicochemical, textural and viscoelastic properties of palm diacylglycerol bakery margarine during storage. Journal of the American Oil Chemists' Society 86(8): 723-731.

Cheong, L.-Z., Tan, C.-P., Long, K., Yusoff, M. S. A., Arrifin, N., Lo, S.-K. and Lai, O.-M. 2007. Production of a diacylglycerol-enriched palm olein using lipase-catalysed partial hydrolysis: optimisation using response surface methodology. Food Chemistry 105(4): 1614-1622

Choo, Y. M. 2012. Malaysia: economic transformation advances oil palm industry. Retrieved on January 20, 2018 from AOCS website: https://www.aocs.org/stay-informed/inform-magazine/featured-articles/malaysia-economic-transformation-advances-oil-palm-industry-september-2012

D'Alonzo, R. P., Kozarek, W. J. and Wade, R. L. 1982. Glyceride composition of processed fats and oils as determined by glass capillary gas chromatography. Journal of the American Oil Chemists' Society 59(7): 292-295.

deMan, J. M. 1999. Relationship among chemical, physical and textural properties of fat. In Widlak, N. (ed.). Physical properties of fats, oils, and emulsifiers. Champaign: AOCS Press.

deMan, L., deMan, J. M. and Blackman, B. 1989. Polymorphic behavior of some fully hydrogenated oils and their mixtures with liquid oil. Journal of the American Oil Chemists' Society 66(12): 1777-1780.

Flickinger, B. D. and Matsuo, N. 2003. Nutritional characteristics of DAG oil. Lipids 38(2): 129-132.

Guillen, M. D. and Cabo, N. 1997. Characterization of edible oil and lard by Fourier transform infrared spectroscopy. Relationship between composition and frequency of concrete bands in the fingerprint region. Journal of the American Oil Chemists' Society 74(10): 1281-1286.

Humphrey, K. L. and Narine, S. S. 2004. A comparison of lipid shortening functionality as a function of molecular ensemble and shear: crystallization and melting. Food Research International 37(1): 11-27.

Idris, N. A., Berger, K. G. and Ong, A. S. H. 1989. Evaluation of shortenings based on various palm oil products. Journal of Science of Food and Agriculture 46(4): 481-493.

Júnior, O. O. S., Montanher, P. F., Bonafé, E. G., Maruyama, S. A., Carbonera, F., Alberici, R. M., ... and Visentainer, J. V. 2013. Efficiencies of acid and based-catalyzed methylation of vegetable oils by ambient mass spectrometry. Journal of the Brazilian Chemical Society 24(11): 1764-1771.

Latip, R. A., Lee, Y. Y., Tang, T. K., Phuah, E. T., Tan, C. P. and Lai, O. M. 2013. Physicochemical properties and crystallization behavior of bakery shortening produced from stearin fraction of palm-based diacylglycerol blended with various vegetable oils. Food Chemistry 141(4): 3938-3946.

Li, Y., Ma, W. J., Qi, B. K., Rokayya, S., Li, D., Wang, J., ... and Jiang, L. Z. 2014. Blending of soybean oil with selected vegetable oils: Impact on oxidative stability and radical scavenging activity. Asian Pacific Journal of Cancel Prevention 15(6): 2583-2589.

Lo, S.-K., Tan, C.-P., Long, K., Yusoff, M. S. A. and Lai, O.-M. 2007. Diacylglycerol oil- properties, processed and products: a review. Food and Bioprocess Technology 1(3): 223-233.

Marangoni, A. G. and Lencki, R. W. 1998. Ternary phase behavior of milk fat fractions. Journal of Agricultural and Food Chemistry 46(10): 3879-3884.

Marita, O. and Soni, M. G. 2009. Safety assessment of diacylglycerol oil as an edible oil: A review of the published literature. Food and Chemical Toxicology 47(1): 9-21.

Miklos, R., Zhang, H., Lametsch, R. and Xu, X. 2013. Physicochemical properties of lard-based diacylglycerols in blends with lard. Food Chemistry 138(1): 608-614.

Murase, T., Mizuno, T., Omachi, T., Onizawa, K., Komine, Y., Kondo, H., … and Tokimitsu, I. 2001. Dietary diacylglycerol suppresses high fat and high sucrose diet-induced body fat accumulation in C57BL/6J mice. Journal of Lipid Research 42(3): 372-378.

Ng, S. P., Lai, O. M., Abas, F., Lim, H. K., Beh, B. K., Ling, T. C. and Tan, C. P. 2014. Compositional and thermal characteristics of palm olein-based diacylglycerol in blends with palm super olein. Food Research International 55: 62-69.

Norizzah, A. R., Norsyamimi, M., Zaliha, O., Nur Azimah, K. and Siti Hozarah, M. F. 2014. Physicochemical properties of palm oil and palm kernel oil blend fractions after interesterification. International Food Research Journal 22(4): 1390-1395.

Petrović, Z. S. 2008. Polyurethanes from vegetable oils. Polymer Reviews 48(1): 109-155.

Reyes-Hernández, J., Dibildox-Alvarado, E., Charó-Alonso, M. A. and Toro-Vazquez, J. F. 2007. Physicochemical and rheological properties of crystallized blends containing trans-free and partially

hydrogenated soybean oil. Journal of the American Oil Chemists' Society 84(12): 1081-1093.

Rohman, A., Kuwat, T., Retno, S., Sismindari, Yuny, E. and Tridjoko, W. 2012. Fourier transform infrared spectroscopy applied for rapid analysis of lard in palm oil. International Food Research Journal 19(3): 1161-1165.

Rousseau, D., Marangoni, A. G. and Jeffrey, K. R. 1998. The influence of chemical interesterification on the physicochemical properties of complex fat systems. 2. Morphology and polymorphism. Journal of American Oil Chemists' Society 75(12): 1833-1839.

Saberi, A. H., Beh, B. K., Lai, O.-M. and Miskandar, M. S. 2011. Physico-chemical properties of various palm-based diacylglycerol oils in comparison with their corresponding palm-based oils. Food Chemistry 127(3): 1031-1038.

Saberi, A. H., Tan, C. P. and Lai, O. M. 2011. Phase behavior of palm oil in blends with palm-based diacylglycerol. Journal of the American Oil Chemists' Society 88(12): 1857-1865.

Saitou, K., Mitsui, Y., Shimizu, M., Kudo, N., Katsuragi, Y. and Sato, K. 2012. Crystallization behavior of diacylglycerol-rich oils produced from rapeseed oil. Journal of American Oil Chemists' Society 89(7): 1231-1239.

Tan, C. P. and Che Man, Y. B. 2000. Differential scanning calorimetric analysis of edible oils: Comparison of thermal properties and chemical composition. Journal of the American Oil Chemists' Society 77(2): 143-155.

Tan, C. P. and Che Man, Y. B. 2002. Differential scanning calorimetric analysis of palm oil, palm oil-based products and coconut oil: Effects of scanning rate variation. Food Chemistry 76(1): 89-102.

Tsimidou, M., Macrae, R. and Wilson, I. 1987. Authentication of virgin olive oils using principal component analysis of triglyceride and fatty acid profiles: Part 1- Classification of Greek olive oils. Food Chemistry 25(3): 227-239.

Xu, X., Kristensen, J. B. and Zhang, H. 2007. Production of novel lipids with functional and health benefits. In Rastall, B. (ed.). Novel enzyme technology for food applications, p. 270-284. Cambridge: Woodhead Publishing.

Xu, Y., Wei, C., Zhao, X., Lu, C. and Dong, C. 2015. A comparative study on microstructure, texture, rheology, and crystallization kinetics of palm-based diacylglycerol oils and corresponding palm-based oils. European Journal of Science and Technology 118(8): 1179-1192.

Yasukawa, T. and Katsuragi, Y. 2004. Diacylglycerols. In Katsuragi, Y., Yasukawa, T., Matsuo, N., Flickinger, B. D., Tokimitsu, I. and Matlock, M. G. (eds.). Diacylglycerol oil, p. 1-15. Champaign: AOCS Press.

Yeoh, C. M., Phuah, E. T., Tang, T. K., Siew, W. L., Abdullah, L. C. and Choong, T. S. Y. 2014. Molecular distillation of diacylglycerol-enriched palm olein and characterization of purified diacylglycerol fractions. European Journal of Lipid Science and Technology 116(12): 1654-1663.